Supporting Information

CO_2 in 1-butyl-3-methylimidazolium acetate

I- Unusual solubility investigated by Raman spectroscopy and DFT calculations

M. Isabel Cabaço[a], M. Besnard[b*], Y. Danten[b], J. A. P. Coutinho[c]

[a] Centro de Física Atómica da UL, Av. Prof. Gama Pinto 2, 1694-003 Lisboa and Departamento de Física, Instituto Superior Técnico, UTL, Av. Rovisco Pais 1049-001 Lisboa, Portugal.

[b] Institut des Sciences Moléculaires, CNRS (UMR 5255), Université Bordeaux 1, 351, Cours de la Libération 33405 Talence Cedex, France.

[c] CICECO, Departamento de Química, Universidade de Aveiro 3810-193 Aveiro, Portugal

[*] Corresponding author: M.Besnard, tel +33 5 40006357, fax +33 5 4000 8402, e-mail: m.besnard@ism.u-bordeaux1.fr

SI.1. Raman spectra of the pure IL and its assignment

The polarised and depolarised spectra of the pure Bmim Ac are displayed in the relevant spectral domains in Figure SI1.

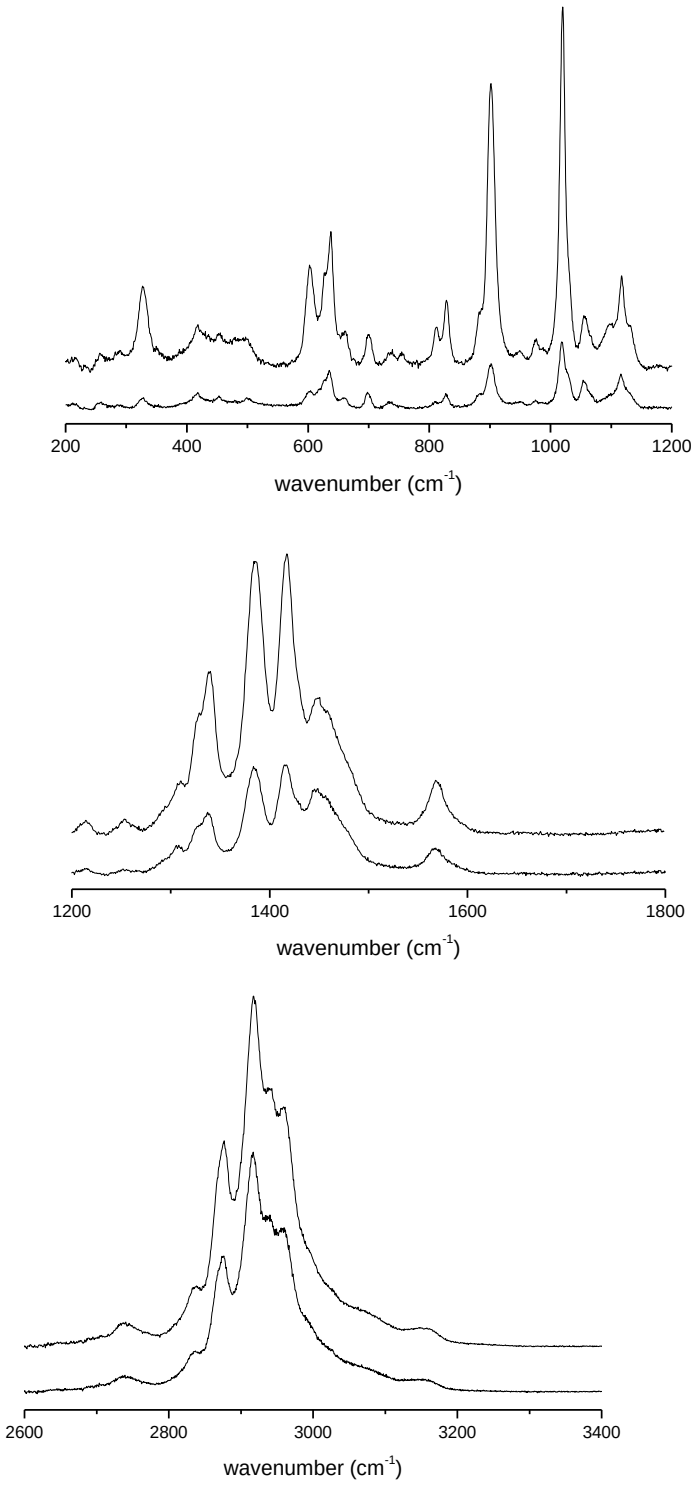

Figure SI1. Polarised VV (top) and depolarised HV (bottom) Raman spectra of pure Bmim Ac. For the clarity of the representation the spectral domain has been split in three regions.

SI.1.1. Cation bands

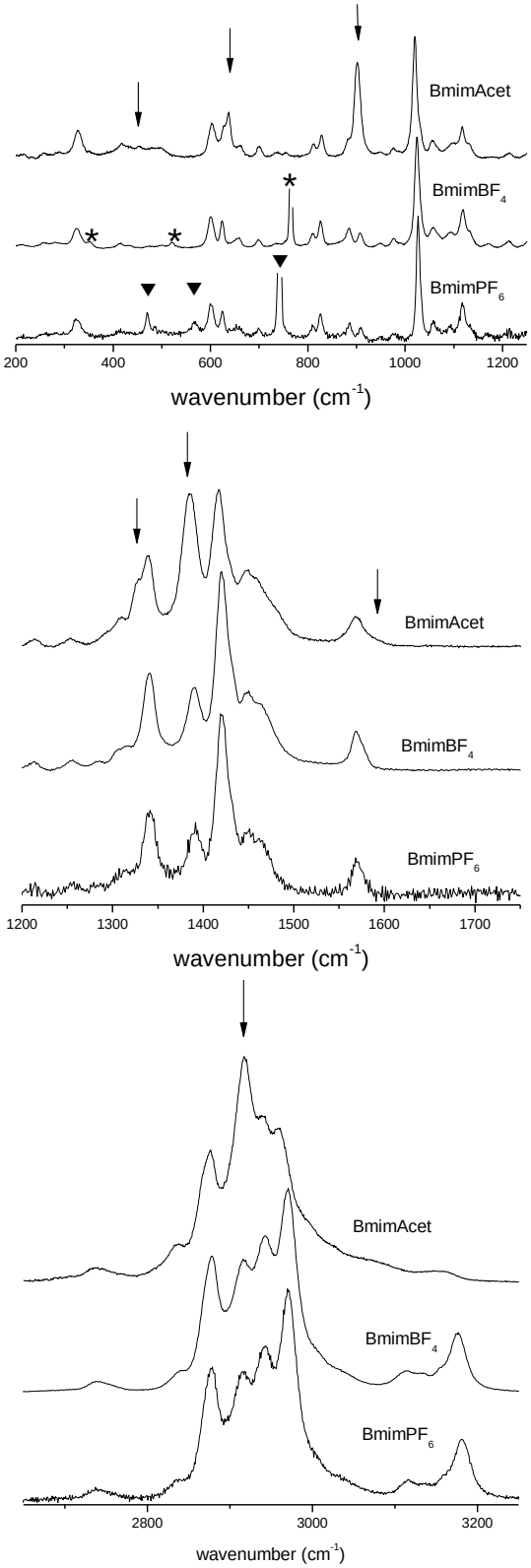

Figure SI2. Comparison of the polarised Raman spectra of pure ionic liquids having the $Bmim^+$ cation in common. The bands of the anions are pinpointed for acetate anion and labelled with (*) BF_4^- and (▼) PF_6^-. For the clarity of the representation the spectral domain has been split in three regions.

Domain 200 cm^{-1}-1800 cm^{-1}

The bands of the cation have been identified based upon a comparison of the polarised spectrum with those of the $Bmim^+$ BF^-_4 and $Bmim^+$ PF^-_6 ionic liquids using the method previously reported (Figure SI2) [1]. The values of the band centre frequency extracted from this procedure and their assignments agree reasonably well with the vibrational frequencies reported as well as in the literature [2-11] and are presented in Table SI1.

Domain 2700 cm^{-1}-3070 cm^{-1}

The assignment of this spectral domain, in which the CH stretching vibrations of the alkyl groups of the Bmim cation and of the methyl group of the acetate anion are active, is made easier by comparison with Bmim TFA. The polarised Raman spectra of Bmim Ac and Bmim TFA are displayed in Figure SI3a.

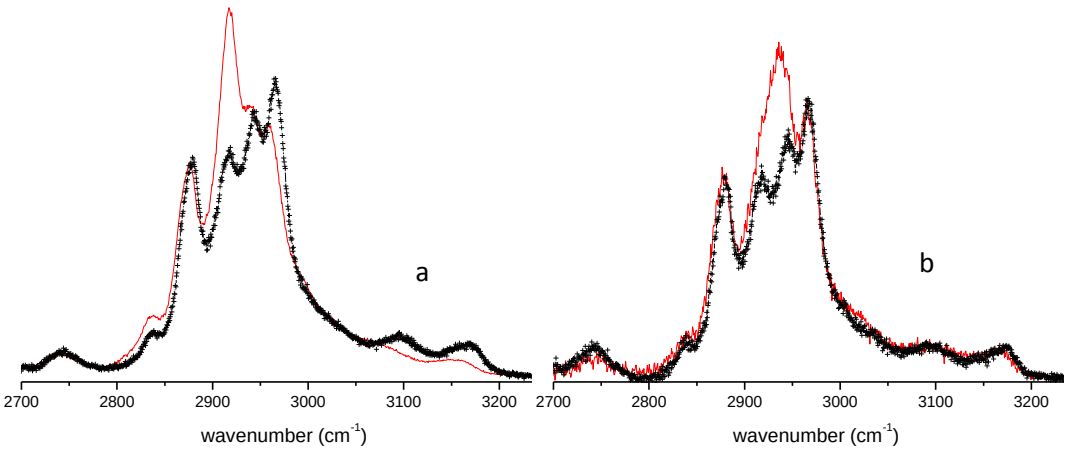

Figure SI3 Comparison of polarised Raman spectra in the domain of the CH stretching vibrations of Bmim acetate (—) and Bmim TFA (+): a) in the pure ionic liquids; b) in the binary with CO_2 mixtures, x CO_2=0.49 in CO_2- Bmim Ac and x CO_2=0.54 in CO_2- Bmim TFA.

We have shown previously (Figure 2c [1]) that the spectra of Bmim TFA, Bmim BF_4, Bmim PF_6 are similar in the domain 2700 cm^{-1}- 3070 cm^{-1}. Hence, the signatures of the CH vibrations of the Bmim cation are not significantly affected by the presence of the anion. In contrast, the comparison of the spectrum of Bmim Ac with that of Bmim TFA shows two major differences. In Bmim Ac, the band situated at 2917 cm^{-1} is strongly enhanced whereas the intensity of the band at 2961 cm^{-1} has a weaker intensity (Figure SI3a). Clearly, the difference between the

spectra of the two ionic liquids in this domain should result partly from the contribution of the methyl band of the acetate ion.

Indeed, from the bandshape analysis of the profile a band centred at about 2917 cm^{-1} can be assigned partly to the symmetrical vibration of the methyl group (Table SI1).

Domain 3070 cm^{-1}-3250 cm^{-1}

We observe two weak features, centred at 3074 cm^{-1} and 3150 cm^{-1}. These bands are markedly weaker and red shifted (by about 45 cm^{-1} and 25 cm^{-1}, respectively) compared to the corresponding ones in Bmim BF_4 and Bmim PF_6 (Figure SI2c). Their assignment is given in Table SI1.

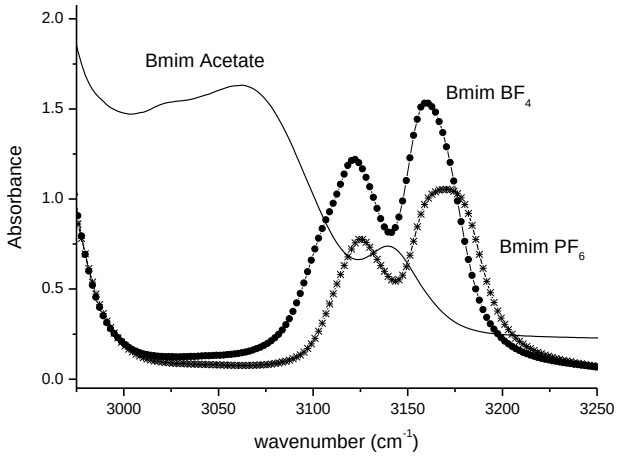

Figure SI4. Comparison of the infrared spectra in the region of the CH stretching vibrations of Bmim Ac (—) with those of Bmim BF_4 (—●—) and Bmim PF_6 (—*—).

In the infrared spectrum of Bmim Ac a composite and significantly distorted band is observed at 3070 cm^{-1} and another at 3144 cm^{-1}. These bands are red shifted by about 50 cm^{-1} and 25 cm^{-1}, respectively, compared with the corresponding ones in Bmim BF_4, values similar to those previously found in Raman (Figure SI4). The intensity ratio of the composite band versus the other is about 13 whereas this ratio is less than unity in both Bmim BF_4 (~ 0.9) and Bmim PF_6 (~ 0.4). The total intensity of these bands is greater than that in Bmim BF_4 and Bmim PF_6 by a factor greater than 1.9. The greater shift and the greater total intensity in Bmim Ac compared to Bmim BF_4 indicate that a greater strength of interaction exists between the ions in Bmim Ac than in Bmim BF_4 and Bmim PF_6 [11]. These bands in Bmim TFA are detected at 3085 cm^{-1} and 3147 cm^{-1}, therefore red-shifted compared with those of Bmim BF_4 but less than those of Bmim Ac,

indicating that the interaction between the carboxylate anion and the Bmim cation is stronger in Bmim Ac than in Bmim TFA.

SI.1.2. Anion bands

We have identified the characteristic bands of the acetate anion, denoted by arrows in Figure SI2, by excluding the bands associated with the cation. To confirm this procedure, we have then measured the Raman spectra of sodium acetate in aqueous solution (1 mol dm^{-3}) presented in Figure SI5 (top). We notice that the frequencies of the bands of the anion in aqueous solution are in good agreement with those reported in the literature under similar conditions [12-19]. In the same figure, the spectrum of Bmim Ac is displayed and the comparison shows that there is a perturbation of the bands position of the anion on going from the aqueous solution to the ionic liquid. This perturbation could be anticipated because the counter-ions are different, as we have found for the system Bmim TFA in comparison with sodium trifluoro acetate [1].

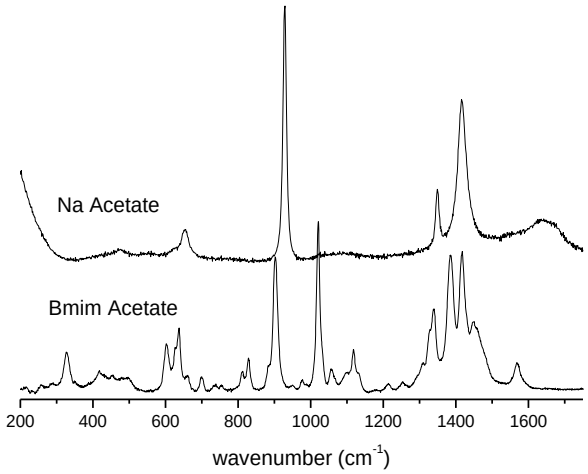

Figure SI5. Comparison of the polarised Raman spectra of Bmim Ac (bottom) and of a one mol dm^{-3} sodium acetate aqueous solution (top).

As the spectral domain 1200 cm^{-1} - 1800 cm^{-1} plays a particularly relevant role in this study and as the bands of the cation and of the anion are somehow overlapping, the disentanglement and attribution of the bands in this region requires a special attention. Hence, we have firstly, compared the Raman spectrum of the ionic liquid in this domain with that of Bmim BF_4 (Figure SI6, top). We observed that the band situated at 1339 cm^{-1} exists also in the Bmim BF_4, whereas the band at 1326 cm^{-1} only appears in the Bmim Ac. We assign this latter band to the δ CH_3 mode of the acetate anion (Table SI1) and the first band to the Bmim cation. The band centred at

about 1385 cm^{-1} in Bmim Ac is observed in the Bmim BF_4 at about the same frequency i.e. 1390 cm^{-1}, but after scaling the two spectra, we see that the intensity of this band in Bmim Ac is more intense and broader. A bandshape analysis using Lorentzian profiles shows that the band observed in Bmim Ac is composite and results from the overlap of two bands centred at 1390 cm^{-1} and 1382 cm^{-1}, the former having an intensity quite comparable to that observed in Bmim BF_4. Thus, we attribute the band at 1390 cm^{-1} to the ν_{CCCC} mode of the Bmim cation and the other to the symmetric stretch of the carboxylate group of the acetate anion[2,5] (Table SI1). The band observed in Bmim Ac at 1568 cm^{-1} is also composite and results from the overlap of a band of the Bmim cation situated at 1568 cm^{-1} (ring modes R1, R2 also present in the spectra of Bmim BF_4) with a very weak band of the acetate anion situated at 1582 cm^{-1} which distorts the high frequency wing of the band of the cation. This very weak band can be assigned to the asymmetric stretch of the carboxylate group [2,5] (Table SI1). To ground definitively, this assignment, we have subsequently used infrared absorption spectroscopy (IR). The comparison of the Raman spectrum of Bmim Ac with the IR spectra shows that this band is clearly observed at about 1580 cm^{-1} due to its strong IR activity (Figure SI6, bottom). Incidentally, the carboxylate symmetric mode although less IR active, is found to overlap with the band observed at 1385 cm^{-1}. The tentative assignment of the bands of the acetate anion in the IL is presented in Table SI1.

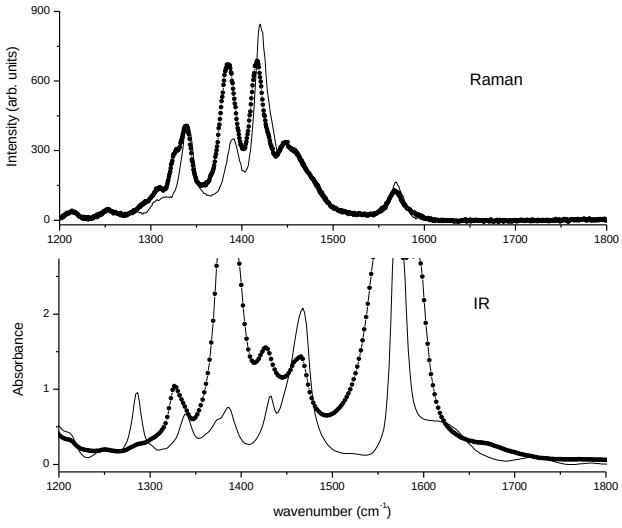

Figure SI6. Comparison of the spectra of Bmim Ac (—●—) and Bmim BF_4 (—) in the region of the carboxylate stretching vibrations: Raman (top) and infrared (bottom).

SI.2. Perturbation of the IL spectrum

Domain 200-1200 cm^{-1}

The main perturbations observed in this domain concern the decreasing of the intensity of the δ COO (637 cm^{-1}) and of the ν_{C-C} vibration (902 cm^{-1}) of the acetate anion as well as the band situated at 1020 cm^{-1} assigned to the coupled in plane ring mode and chain modes of the Bmim cation (Figure 2a). A new and very weak peak centred at about 794 cm^{-1} is also detected. Finally, the intensity of the band situated at 1020 cm^{-1} strongly decreases (by about a factor 2) as the CO_2 concentration increases in the mixture.

Domain 1200-1800 cm^{-1}

The strongest perturbations of the spectrum of the IL are observed in this domain in which the spectral signature of CO_2 is detected (Figure 2b). The three overlapping peaks situated at 1307 cm^{-1} (not attributed), 1326 cm^{-1} (δ CH_3 of the acetate) and 1339 cm^{-1} (CN stretching modes of the methyl and methylene groups bonded to the nitrogen atoms coupled with the in-plane ring symmetric stretch modes of the cation, Table SI1) have their intensity enhanced and we notice that the gap, situated at 1315 cm^{-1}, between the first two bands is progressively filled as the pressure increases. The intensity of the peak centred at about 1447 cm^{-1} (symmetric in-plane ring) dramatically increases and its band centre is red shifted, by about 5 cm^{-1} as soon as the IL is diluted ($x_{CO_2} > 0.23$). In contrast, the intensity of the composite line situated at 1385 cm^{-1} decrease until x_{CO_2} is about 0.35, concentration at which a narrow band appears at about 1380 cm^{-1} which is assigned to the upper component of the Fermi dyad. We notice that the intensity of the band at 1416 cm^{-1} (asymmetric in-plane ring) decreases and that the intensity of the weak band situated at 1582 cm^{-1}, assigned to asymmetric stretch of the carboxylate group vanishes with the pressure. Finally, two new bands, which are absent in the pure IL, are detected at about 1672 cm^{-1} and 1510 cm^{-1}, the last one being extremely weak.

Domain 2700-3070 cm^{-1}

The polarised Raman spectrum corresponding to this domain is displayed in Figure SI3b and the main perturbations observed concern the peaks centred at 2917 cm^{-1} and 2940 cm^{-1}. The intensity of the former peak decreases with the CO_2 concentration, whereas the intensity of the latter peak is enhanced. These peaks collapse for $x_{CO_2} \sim 0.25$ leading to a broad line centred at about 2929 cm^{-1} which is then slightly blue shifted with an increasing CO_2 concentration. In contrast, the

peaks at 2874 cm^{-1} having a shoulder at 2866 cm^{-1}, are not affected by the dilution whereas the peak situated at 2961 cm^{-1} is slightly blue shifted (≈ 7 cm^{-1}). Finally, we note the enhancement of a weak and broad feature at about 3025 cm^{-1} which is barely detected in the pure IL and clearly observed at high CO_2 content. A bandshape analysis of the composite band reveals the existence, among others, of an intense band situated at about 2936 cm^{-1} assigned to methyl symmetrical vibration of the acetate (Table SI1). We note that the corresponding band detected in the pure IL at 2917 cm^{-1} is red-shifted compared to the band in the mixture. This result suggests that the interaction between the ions is weaker in the mixture than in the IL. The value of this band position is the same than that obtained for an aqueous solution of Na Ac (Table SI1).

In the spectral domain of the CH stretching vibrations using the same procedure previously reported, by adding to the spectrum of pure Bmim TFA, the spectrum of the acetate anion, we have succeeded to reproduce the spectrum of the most diluted mixture in Bmim Ac (x_{CO_2} = 0.49) but now without shifting the spectrum of the acetate anion. The intensity of the peaks at 2917 cm^{-1} and 2968 cm^{-1} are now correctly reproduced. A progressive blue shift of the spectrum of the acetate anion is able to reproduce the spectra measured at intermediate dilutions. It comes out that the interaction between the Bmim cations and the acetate anions is strongly weakened upon dilution although the CH vibrations of the imidazolium cation do not appear significantly perturbed.

The other main perturbations of the spectra concern the band at 2960 cm^{-1} which results from the overlap of the asymmetric stretch of the terminal methyl group of the alkyl chain and of the symmetric stretch of the methyl bonded to the imidazolium ring (N-CH_3) (Table SI1). As the bands associated with the methylene groups of the alkyl chain are not perturbed by the dilution we may conclude that this result should apply to the terminal methyl group. Therefore, we may infer that it is the ring which is mostly perturbed. The viewpoint of a perturbation more localised on the ring than on the alkyl chain is reinforced by noting that the bands at 3027 cm^{-1} (N-CH_3 of the symmetric stretch of the methyl bonded to the imidazolium ring) and 2833 cm^{-1} (overtone of the ring vibration) are also affected by the dilution. Similarly, we remind that the peak observed at 417 cm^{-1} assigned to the bending N-CH_3 supports this view (Table SI1).

Domain 3070 cm^{-1}-3250 cm^{-1}

The intensity of the weak feature observed at 3150 cm^{-1} in the pure IL is enhanced and slightly blue shifted whereas the weak band centred at 3074 cm^{-1} is blue shifted (about 25 cm^{-1}) keeping almost the same intensity with dilution in carbon dioxide (Figure 2c, bottom) as indicated by a

band-shape analysis. These trends are confirmed by the comparison of the infrared spectra of the pure IL with a very diluted mixture (see section II.2.2) (Figure SI7). Finally, we found that the Raman spectra of the diluted Bmim Ac (x_{CO_2} = 0.49) in this spectral domain is almost identical to that of pure Bmim TFA. This finding shows that the strength of interaction between the ions is weakened by the dilution effect in CO_2.

The assignment of the bands centred at 3074 cm^{-1} and 3150 cm^{-1} has been the object of discussion. It is generally accepted that the former corresponds to the C(2)H stretching vibration whereas the latter corresponds to the C(4)H and C(5)H in plane and out plane stretching vibrations of the CH group of the ring. Recently, it has been proposed that the high frequency vibration could be assigned to the all the previous CH stretching vibrations and that the band at lower frequency results from the Fermi resonance of the overtones 2R1 and 2R2 of the ring modes with the combination R1+R2 [9]. Because we found that the band at 3150 cm^{-1} is very little affected by the dilution, we can infer on the ground of both assignments, that the C(4)H and C(5)H in plane and out plane stretching vibrations of the CH group of the ring are not affected by the interaction with carbon dioxide. It is more difficult to conclude about the origin of the perturbation observed on the band situated at lower frequency. Nevertheless according to the first assignment, we may infer that it is the third C(2)H group of the ring which is perturbed. Using the second type of assignment, we are led to conclude that the perturbation mostly affects the R1 and R2 vibrations of the ring and that this effect is observed indirectly through the Fermi resonance coupling. Taking into account this conclusion and the two above assignments, we can infer that the perturbation mostly concern the ring core. Although, we cannot discriminate between the two assignments, we note that they are consistent with our previous conclusion that the alkyl chain is not so affected by the interactions as it is for the ring core.

Perturbation of the Bmim Acetate at very low CO_2 concentration

Because the spectrum of Bmim Ac is strongly affected as soon as carbon dioxide is mixed with the IL, we have conducted further experiments at lower CO_2 pressure in view to better characterise the perturbations observed on the IL. In particular, we wanted to assess the formation of the reversible complex and the possible existence of the chemical reaction between CO_2 and the IL at very low pressure (less than 0.1 MPa) as discussed by Shiflett et al [20]. For this purpose, the pure IL was stored in a glass container connected to a vacuum line and properly degassed and dried during several days before introducing CO_2 under a pressure of 0.1 MPa.

After a waiting time of several hours, to let a possible reaction to occur, the line was evacuated and a degassing process, under a residual vacuum pressure of ~10^{-2} Torr lasting for more than 24 hours, was started. This procedure was repeated several times (up to seven cycles) and after each cycle, the container was brought to the Raman spectrometer for examination. We have compared the spectrum of the mixture corresponding to the last cycle discussed above to that of the pure IL (Figure SI7, top). A glance at this figure shows that the perturbations observed on the spectra at high pressure (Figure 2b) are still detected without the signature of the Fermi dyad of CO_2. Afterwards, we have checked the effect of the temperature by heating the mixture up to 363 K during more than twelve hours. We noticed that the intensity of the modes observed at about 1450 cm^{-1} and 1670 cm^{-1} decreased but do not vanish and were still detected (Figure SI7, top). The transmission infrared spectrum of heated mixture confirmed the existence of the new band observed at about 1670 cm^{-1}(absent in the pure IL), strongly active in infrared as well as the strong enhancement of the band at about 1325 cm^{-1} (Figure SI7, bottom). A weak band at about 1510 cm^{-1} and a weak and narrow band at about 2337 cm^{-1} which have not been observed in the Raman spectrum were also detected in the IR spectrum.

It is noteworthy that these bands detected in IR have been already reported by Shiflett et al [21] but not assigned. In contrast, to these authors, these new bands are still detected in the Raman and IR spectra of the mixture heated (at higher temperature 363 K compared with 352 K).

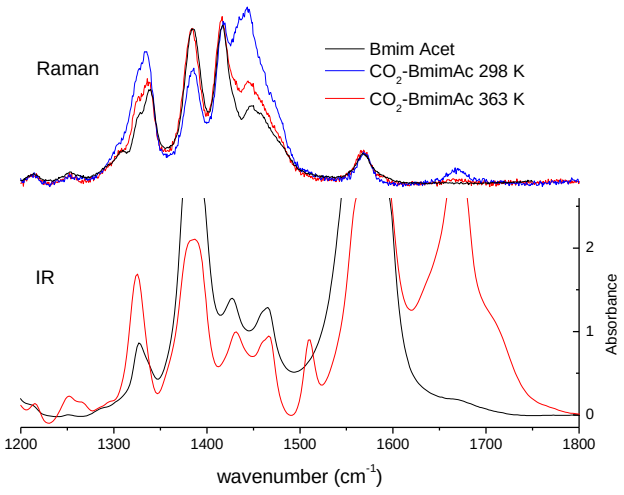

Figure SI7. Comparison of the polarised Raman (top) and infrared (bottom) spectra of pure Bmim Ac with those of its binary mixtures with carbon dioxide at 0.1 MPa

SI.3. Vibrational modeling using DFT calculations

SI.3.1. Structures and interaction energy

The Pure IL

In a first step, we have determined the global energy minimum structure for the pure ionic liquid modelled as a ion pair dimer IP2 $\{Bmim\ Ac\}_2$ (Figure SI8).

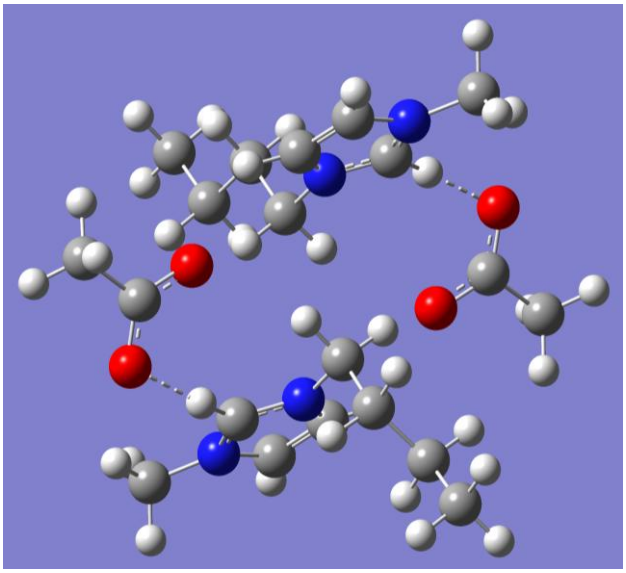

Figure SI8.-Structure I calculated at the B3LYP/6-31+G** level for the ion pair dimer

In this structure (I), one oxygen atom of each acetate anions is coordinated with the proton in C_2 position of each imidazolium cations. This structural organization involves two of the so-called single interactions (monodendate form) according to the nomenclature used by Bowron et al [22]. The calculated interatomic distances between the two coordinated atoms $R_{O..HC(2)}$ are about 1.75-1.76 Å. We notice that in this structure, secondary interactions between acetate oxygen and ring hydrogen atoms in position either in C_4 or C_5 positions are also involved with interatomic O..H distances about 2.14-2.16Å. The BSSE-corrected values of the different contributions to the total interaction energy (ΔE_{int}(ions) ~ -216.5 kcal/mol) are reported in Table SI2. In this structure, the non additive contribution (irreducible 3- and 4-bodies) to the interaction energy represents globally a repulsive contribution about 15% of the total interaction energy.

Other possible secondary IP2 structures (but less stable) involving possibly other types of coordination such as bifurcated, bridging or multiple interactions between acetate oxygen atoms and ring hydrogen atoms have not been straightforwardly found from the examination of the IP2 potential energy surface and have not been further considered here. Indeed, the IP2 structures

calculated here are more related with a description of the interactions within the polar regions of the IL. However, the so-called bidendate interactions (i.e. both acetate oxygens close to one hydrogen atom of the imidazolium cation as defined in the structural analysis carried out by Bowron et al [22]) have not been found from our DFT calculations. Indeed, such structures should involve O…H interionic distances slightly greater than in single interactions [22] whereas our methodology allows us assessing more easily short-ranged structures. However, we have determined structures IP2 in which one of the two ion pairs involves a very short-ranged specific cation-anion interaction. In this specific IP sub-structure, both acetate oxygen atoms interact with two hydrogen atoms of the imidazolium cations. The former oxygen interacts with the acid proton of the cation (interatomic O…H distance about 1.647 Å) and the latter oxygen interacts with one of the hydrogen atom of the CH_3 group bounded to the N(3)-atom of the imidazolium ring. (interatomic O…H distance about 2.005 Å). It is noteworthy that the C_2 H-bond is found strongly polarized in this short-ranged IP structure (bond-length about 1.135 Å).

The mixture CO_2 – Bmim Acetate

We have determined the most stable structure representative of a (low CO_2 concentrations) mixture idealized by a CO_2 molecule interacting with the $(IP)_2$ $\{Bmim\ Ac\}_2$ (Figure SI9).

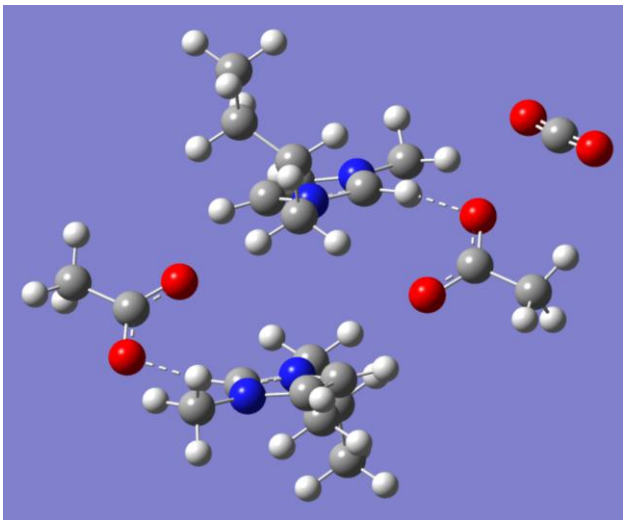

Figure SI9. Structure II calculated at the B3LYP/6-31+G** level for the ion pair dimer interacting with a CO_2 molecule.

In the resulting structure (II), the C atom of CO_2 interacts with one of the two O atoms of the COO^- group of an acetate anion (interatomic distance $R_{C..O}$ about 2.66 Å). Notice that the structural organisation between the ions is few affected by the presence of CO_2. The calculated interaction energy between CO_2 and the ion pair is - 4.8 kcal/mol (Table SI2). As expected, the

presence of CO_2 has a minor influence on the stability between ions (<1 kcal/mol). Therefore, the interaction of CO_2 with the ions $\Delta E_{int}(CO_2\text{-ions})$ represents the main stabilizing contribution to the total energy variation under the complex formation of CO_2 with $(IP)_2$. The non additive (3-body) interaction energy $\Delta E_{int}^{(3)}$ between CO_2 and the $\{Bmim\ Ac\}_2$ represents a destabilizing (repulsive) contribution about +3.0 kcal/mol. Thus, from such a 'gas phase model' we can evaluate the association energy of CO_2 with the $\{Bmim\ Ac\}_2$ ΔE_f (CO_2) about -4.8 kcal/mol. We have also reported in (Table SI2) the corresponding estimate of the enthalpy variation ΔH_f (CO_2) under the complex formation calculated at 298 K and 1 atm. Finally, it is also noteworthy that the interaction site for CO_2 is found with the acetate oxygen which is itself involved in the single interaction with the acidic proton of the imidazolium ring.

Compared with our previous DFT calculations about CO_2 interactions with $\{Bmim\ TFA\}_2$ [1], we notice that the strength of interionic interactions is found to be higher with Ac anions than as TFA anions are involved. Indeed, we evaluate ΔE_{int}(ions) at about -193 kcal/mol for the calculated structure $\{Bmim\ TFA\}_2$ (with and without CO_2) instead of -216.5 kcal/mol with Ac anions. In the same way, CO_2 interactions with TFA anions are also found less attractive than with Ac ones with an interaction energy $\Delta E_{int}(CO_2\text{-ions})$ about -3.6 kcal/mol (with association energy ΔE_f (CO_2) and formation enthalpy ΔH_f (CO_2) -3.3 and -2.6 kcal/mol, respectively. Nevertheless, it is noteworthy that at this computational level (B3LYP/6-31+G**) the difference found between the estimated values of the interaction energy of CO_2 with ionic species in the structures $\{Bmim\ Ac\}_2$ and $\{Bmim\ TFA\}_2$ is relatively weak (~1 kcal/mol).

SI.3.2. Vibrational Analysis

We have carried out the vibrational analysis of the predicted $(IP)_2$ structures without and with CO_2, I and II, respectively. The main calculated (harmonic) fundamental transitions, the IR and Raman Intensities (as well as the depolarization ratios) are reported in Table SI3. This table shows that globally the vibrational modes of both ionic species are slightly perturbed by the presence of CO_2. However, we notice some spectral differences upon vibrational modes of CO_2 interacting with one of the O atom of the COO group of an anion (Structure II).

The calculated frequency associated with the ν_{CC} stretching modes, the $\nu^{(s)}_{COO}$ symmetric and $\nu^{(as)}_{COO}$ asymmetric stretches of acetate anions and the IR and Raman intensities corresponding to these transitions are only weakly perturbed by the introduction of CO_2 (structure II) (Table

SI3). It is well-established that the frequency separation $\Delta\nu_{COO}=|\nu^{(as)}_{COO}-\nu^{(s)}_{COO}|$ between the symmetric and the asymmetric stretches of the carboxylate group of metal-coordinated acetates in aqueous solutions is strongly correlated with the interaction strength existing in different types of coordination of the acetate [23-25]. Thus, the variation of $\Delta\nu_{COO}$ is considered as a spectral signature of the interaction of the anion species in its environment. The smallness of $\Delta\nu_{COO}$ leads us to conclude that the $(IP)_2$ structural organization is not perturbed by CO_2 in structure II.

Considering the carbon dioxide, the most perturbed mode is the ν_2 OCO bending in which the degeneracy of this mode is raised and it is split in two components (resp. $\nu_2^{(1)}$ and $\nu_2^{(2)}$). The splitting $\Delta\nu_2=|\nu_2^{(2)}-\nu_2^{(1)}|$ is related with the perturbations applied on CO_2 by its environment. In the structure II, the splitting is about 51 cm^{-1} (Table SI3). The IR intensity of the lowest frequency component is significantly enhanced under the complex formation whereas that of the highest frequency component decreases. In Raman, the activity of this mode is interaction-induced (unauthorized transitions) and mainly distributed on the lowest frequency $\nu_2^{(1)}$ component of this mode. Such specific IR and Raman spectral signatures on the ν_2 mode of CO_2 should clearly indicate the Lewis acid-base nature of the CO_2-anion interaction. However, experimentally, the existence of well-defined bands due to ionic species in IL hampers the detection of a possible weak and broad Raman bands due to the ν_2 bending mode of CO_2. Moreover, the frequency values calculated for the bending and asymmetric stretch vibration are found significantly different from the corresponding vibrations of CO_2 detected in the first solvation regime (Table SI3) which are characteristic of a C coordinated CO_2.

In summary, the structural description reported here does not reveal any major difference with those reported for CO_2 diluted in Bmim TFA [1]. In this context, let us remind that the interaction of CO_2 with the Ac and TFA anions have been studied by DFT and ab-initio (at the MP2 level) calculations [26]. The aim of this study was to provide insight on the solvation of CO_2 in IL containing these anions on an energetic basis in an idealised manner consisting in the complete neglect of the presence of the imidazolium cation. The features reported for these two systems (minimum approach distances and binding energy of the complex, OCO angle of CO_2 and splitting of its bending mode), show that the interaction of CO_2 is greater with the Ac anion. Although, this conclusion is qualitatively in agreement with the work discussed here, we found that all the features reported by the authors are strongly overestimating those reported in the current study on Bmim Ac and with Bmim TFA. For instance, this can be illustrated by the values of the interaction energy of CO_2 with the anion which are found to be -8.37 kcal $mole^{-1}$ and -5.74 kcal $mole^{-1}$ in Ac and TFA, respectively. These values are clearly much greater than

those reported in Table SI2. This is not surprising as calculations only taking into account the interaction between two bodies, neglecting the cation contribution and not considering a realistic ionic environment are better adapted to a treatment of gas phase clusters (as proposed by the authors) and should be only extrapolated with great caution to the discussion of the solvation in IL.

So, we conclude that the schemes and hypotheses used, also considering a realistic ionic environment, are rather inadequate for providing a realistic description of the nature of the interactions of CO_2 involved in the first solvation regime of CO_2 existing in Bmim Ac. For this reason, we will tackle the question of the carboxylation in a more effective way in the following.

References

(1) Cabaço, M. I.; Besnard, M.; Danten, Y.; Coutinho, J. A. P. *J Phys Chem B* **2011**, *115*, 3538.

(2) Talaty, R.; Raja, S.; Storhaug, V. J.; Dölle, A.; Carper, W. R. *J. Phys. Chem. B* **2004**, *108*, 13177.

(3) Berg, R. W.; Deetlefs, M.; Seddon, K. R.; Shim, I.; Thompson, J. M. *J. Phys. Chem. B* **2005**, *109*, 19018.

(4) Rivera-Rubero, S.; Baldelli, S. *J Phys Chem B* **2006**, *110*, 4756.

(5) Heimer, N. E.; Sesto, R. E. D.; Meng, Z.; Wilkes, J. S.; Carper, W. R. *J. Mol. Liq.* **2006**, *124*, 84.

(6) Holomb, R.; Martinelli, A.; Albinsson, I.; Lassègues, J. C.; Johansson, P.; Jacobsson, P. *Journal of Raman Spectroscopy* **2008**, *39*, 793.

(7) Jeon, Y.; Sung, J.; Kim, D.; Seo, C.; Cheong, H.; Ouchi, Y.; Ozawa, R.; Hamaguchi, H.-o. *J Phys Chem B* **2008**, *112*, 923.

(8) Jeon, Y.; Sung, J.; Seo, C.; Lim, H.; Cheong, H.; Kang, M.; Moon, B.; Ouchi, Y.; Kim, D. *J Phys Chem B* **2008**, *112*, 4735.

(9) Lassègues, J.-C.; Grondin, J.; Cavagnat, D.; Johansson, P. *J Phys Chem A Letters* **2009**, *113*, 6419.

(10) Wulf, A.; Fumino, K.; Ludwig, R. *J Phys Chem A* **2010**, *114*, 685.

(11) Lassègues, J. C.; Grondin, J.; Cavagnat, D.; Johansson, P. *J Phys Chem A* **2010**, *114*, 687.

(12) Ito, K.; Bernstein, H. J. *Canadian Journal of Chemistry* **1956**, *34*, 170.

(13) Spinner, E. *J Chem Soc* **1964**, 4217.

(14) Kakihana, M.; Kotaka, M.; Okamoto, M. *J Phys Chem* **1982**, *86*, 4385.

(15) Paul, I.; Kang, S.; Spinner, E. *Aust J Chem* **1986**, *39*, 465.

(16) Kakihana, M.; Nagumo, T.; Okamoto, M.; Kakihana, H. *J Phys Chem* **1987**, *91*, 6128.

(17) Quilès, F.; Burneau, A. *Vibrational Spectroscopy* **1998**, *16*, 105.

(18) Quilès, F.; Burneau, A. *Vibrational Spectroscopy* **1998**, *18*, 61.

(19) Frost, R. L.; Kloprogge, J. T. *J Molecular Structure* **2000**, *526*, 131.

(20) Yokozeki, A.; Shiflett, M. B.; Junk, C. P.; Grieco, L. M.; Foo, T. *J Phys Chem B* **2008**, *112*, 16654.

(21) Shiflett, M. B.; Kasprzak, D. J.; Junk, C. P.; Yokozeki, A. *J Chem Thermodynamics* **2008**, *40*, 25.

(22) Bowron, D. T.; D'Agostino, C.; Gladden, L. F.; Hardacre, C.; Holbrey, J. D.; Lagunas, M. C.; McGregor, J.; Mantle, M. D.; Mullan, C. L.; Youngs, T. G. A. *J Phys Chem B* **2010**, *114*, 7760.

(23) Deacon, G. B.; Phillips, R. J. *Coordination Chemistry Reviews* **1980**, *33*, 227.

(24) Nakamoto, K. *IR and Raman spectra of Inorganic and Coordination Compounds* 6th ed.Hoboken, New Jersey, 2009; Vol. Part B.

(25) Nara, M.; Torii, H.; Tasumi, M. *J Phys Chem* **1996**, *100*, 19812.

(26) Bhargava, B. L.; Balasubramanian, S. *Chem. Phys. Letters* **2007**, *444*, 242.

(27) Mierzwicki, K.; Latajka, Z. *Chem. Phys. Lett.* **2003**, *380*, 654.

(28) Valiron, P.; Mayer, I. *Chem. Phys. Lett.* **1997**, *1997*, 46.

Table SI1: Tentative assignment of the Raman bands of the acetate anion in Bmim Ac (pure and mixture) and in aqueous solution of sodium acetate (1 mol dm^{-3}). The assignment of the bands of the anion have been taken from [12-19] and for the cation from [2,5,6,9]. Only the perturbed bands of the cation in the mixture are presented here.

Acetate anion				Bmim cation		
xCO2=0	xCO2=0.49	Na Ac	Assignement	xCO2=0	xCO2=0.49	Assignement
				328 (m,P)		b (CH_3 (N), CH_2(N)), δ CCCC
				418(m,P)		b (CH_3 (N), CH_2(N),CH_3)
454 (w,P)	454 (vw)	470 (w,P)	rock // COO			
		557 (w,P)		603 (m,P)		b (ring op), ν iph (CH_2(N), CH_3 (N))
		622 (w,P)	rock ⊥ COO			
637 (m,P)	637 (w,P)	653 (m,P)	b OCO			
				627 (w,P)		b (ring op), ν iph (CH_2(N), CH_3 (N))
				659 (vw)		b Ring op), ν (CH_3(N))
				700 (vw)		ν oph (CH_2(N),CH_3(N))
	794(w,P)		b OCO [a]			
				811 (w,P)		ν sym (chain CC), b iph (ring (HCCH, NC(H)N op)
				828 (m,P)		b iph (ring HCHH, NC(H)N op), ν sym (chain CC)
				882 (m,P)		ν sym ($CH_2CH_2CH_3CCC$)
902 (s,P)	910 (m,P)	928 (vs,P)	ν CC			
				907(w,P)		ν sym ($CH_2CH_2CH_3CCC$)
				1020 (vs,P)	1020 (s,P)	ν (ring CN ip iph, CH_2(N), CH_2CH_3CC)
				1056 (w)		ν asym (chain CCC)
				1096 (w)		b ((N)CH_3CH),ν asym (ring CN)
				1117 (m,P)		ν sym (chain CCC)
				1132(vw)		ν (chain CC), b (butyl CH)
				1307 (sh,w)	1306(sh,m)	
	1323(s,P)		ν sym COO [a]			
1326 (m,P)	1323(s,P)	1349 (m,P)	b CH_3			
				1339 (s,P)	1336(s,P)	ν CH_3 (N),ν CH_2(N),ν sym ip ring
1382 (vs,P)	1381 (s,P)[b]	1417 (vs,P)	ν sym COO			
				1390 (m,P)	1390(m,P)	ν CCCC
				1416 (vs,P)	1417 (m,P)	ν asym ip ring, ν CH_3 (N)
				1429 (w,P)	1433 (m,P)	ν asym ip ring, ν CH_3 (N)
				1447 (m,P)	1445 (vs,P)	ν sym ip ring
				1461 (s,P)	1458 (vs,P)	ν ring CH_3 CN
				1479 (m,P)	1476 (m,P)	
					1510 (vw)	
				1568 (w,P)	1568 (w,P)	ν CH_3(N), ν CH_2(N), ν asym ip ring
1582(sh,w)		1556 (vw) [c]	ν asymCOO			
	1672 (w,D)		ν asymCOO [a]			
				2833 (w,P)	2838(vw,P)	
				2874 (s,P)	2876 (s,P)	ν sym CH_3HCH (terminal), ν sym CH_2C(N)HCH
2917(vs,P)	2936(vs,P)	2936 (vs,P)	ν sym CH_3	2917 (vs,P)	2917 (s,P)	ν asym ethyl HCH
				2941 (m,P)	2939 (vs,P)	ν sym CH_3(N) HCH
				2961 (s,P) [d]	2968(s,P)	ν asym propyl HCH
				2995(m,P)	2999(w,P)	
				3027 (w,D)	3023(m,D)	
				3074 (w,P) [e]	~3097(w,P)	ν asym CH_3(N)HCH [g]
				3150(vw,P) [f]	~3155(w,P)	ν sym ring HCCH, ν NC(H)N CH [g]

The units of frequency are cm^{-1}. P-polarised and D-depolarised profiles; rock ⊥ and rock //, rocking perpendicular and parallel to the CCOO plane; b, bending; ν stretching; sym and asym, symmetric and asymmetric vibrations, respectively; ip and op, in-plane and out-of-plane; iph and oph, in-phase and out-of-phase vibrations, respectively.

[a] new bands (see Table 2)

[b] band contributing to the intense upper component of the Fermi dyad

[c] band contributing to the broad feature observed in the domain of the water bending

[d] 2970 cm^{-1} for Bmim PF_6 and Bmim BF_4

[e] 3120 cm^{-1} for Bmim PF_6 and Bmim BF_4

[f] 3175 cm^{-1} for Bmim PF_6 and Bmim BF_4^-

[g] This assignment is commonly accepted, however it has been revisited recently and a new kind of assignment has been proposed: [d] is assigned to the ν iph $C_{(4,5)}$ H, ν $C_{(2)}$H and ν oph $C_{(4,5)}$ H modes; [e] is assigned to overtones and combination of the ring modes in Fermi resonance [9-11]

Table SI2: BSSE-corrected values of the interaction energy obtained for the IP2 $\{BMI\text{-}Ac\}_2$ structures with and without CO_2 calculated at the B3LYP/6-31+G(p,d) level.

	IP2 $\{BMI\text{-}Ac\}_2$ Structure I	**IP2 $\{BMI\text{-}Ac\}_2+CO_2$ Structure II**
ionic interactions		
$\Delta E_{int}(ions)$	-216.5	-216.0
$\Delta E_{int}^{(2)}$	-246.7	-246.3
$\Delta E_{int}^{(3+4)}$	+30.2	+30.3
CO_2-ion interactions		
$\Delta E_{int}(CO_2\text{-ions})$	-	-4.8
$\Delta E_{int}^{(2)}$	-	-7.8
$\Delta E_{int}^{(3)}$	-	+3.0
total interaction energy		
$\Delta E^{(cor)}_{int}(TOT)$	-216.5	-220.8
$\Delta E_f(CO_2)$	-	-4.5
$\Delta H_f(T_{298K})$	n.c.	-3.5

The units of energy are kcal/mol. Many-bodies interactions have been evaluated according to the SSFC scheme [27,28].

$\Delta E_f(CO_2)$ is the predicted 'gas phase' value of the association energy of CO_2 with $\{BMI\text{-}Ac\}_2$ and $\Delta H_f(T_{298K})$ the corresponding enthalpy of formation calculated at T=298K**.**

Table SI3: Vibrational transitions, IR and Raman intensities associated with the main vibrational transitions of the calculated structures $\{B_{Mim}^{+}/CH_3COO^{-}\}_2$ (I) and $\{B_{Mim}^{+}/CH_3COO^{-}\}_2 + CO_2$ (II) at the B3LYP/6-31+G** level.

	$\{B_{Mim}^{+}/CH_3COO^{-}\}_2$ (structure I)				**$\{B_{Mim}^{+}/CH_3COO^{-}\}_2+CO_2$ (structure II)**			
	ν_{calc}	**I_{IR}**	**I_{Ram}**	**$\rho_{dep.}$**	**ν_{calc}**	**I_{IR}**	**I_{Ram}**	**$\rho_{dep.}$**
b OCO (CO_2)					608	132	22	0.53
					659	25	0.2	0.24
b OCO (Ac)	645	11	8.9	0.28	645	11	7.5	0.26
	646	51	0.9	0.23	648	45	2.9	0.28
ν_{CC} (Ac)	909	7.0	19.9	0.12	913	3.4	18	0.08
	913	73	3.2	0.11	916	75	1.2	0.75
ν sym CO (CO_2)					1358	9.4	41	0.10
sym ip ring	1371	0.2	20.0	0.22	1371	1.2	22.5	0.21
	1372	1.	6.5	0.21	1372	0.8	4.8	0.31
ν sym COO	1425	226	19.7	0.64	1426	264	11	0.73
	1426	220	23.7	0.72	1428	187	38	0.75
sym ip ring	1452	42	23.8	0.18	1451	30.4	33.5	0.17
	1454	17	52.8	0.23	1456	12.3	40.7	0.28
ν asym C(CN) ring	1598	0.8	11.4	0.20	1599	219	7.1	0.15
	1600	455	0	0.44	1605	207	4.5	0.12
ν sym. C(CN) ring	1610	2.4	10.2	0.23	1611	1.2	8.9	0.22
	1615	202	0.3	0.73	1614	48	0.7	0.70
ν asym COO	1622	749	0.05	0.72	1619	823	1.2	0.64
	1625	0.2	6.8	0.65	1624	209	4.9	0.64
ν asym CO (CO_2)					2400	610	0.6	0.73

* vibrational transition of the carboxylate . Values for labelled ^{13}C in the carboxylate group are reported in parentheses (see text). The units of frequency, IR activity and Raman intensity are cm^{-1}, Km/mol and $Å^4$/amu, respectiv